Porosity and Pore Size Determination in Polysulfone Hollow Fibers

I. CABASSO, K. Q. ROBERT, E. KLEIN, and J. K. SMITH, *Gulf South Research Institute, New Orleans, Louisiana 70186*

Synopsis

Average pore sizes and effective porosity of microporous polysulfone hollow fibers were determined by the gas permeability method. Surface structure and porosity were determined by scanning electron microscopy. The values of effective porosity ϵ/q^2 (porosity/tortuosity factor) are approximately one order of magnitude lower than those reported previously for flat sheet porous membrane. These lower values are a direct outcome of a higher polymer concentration in the spinning dope. Correlations between the wall void volume, equivalent pore size, and hydraulic permeabilities of the hollow fibers have been determined. Rather low values of ϵ/q^2 have been calculated compared to those of the void volume; these effective porosity values indicate either a very high tortuosity factor or a large number of "dead end" pores. Exposure of the fibers to elevated temperature (110°C) for a short period of time drastically reduces the surface pore size and narrows the pore size distribution, whereas overall fiber dimensions are reduced only by 1%, and 85% of the fiber's hydraulic permeability is retained. The scanning electron microscopy study reveals the formation of a relatively dense skin in some spun fibers. For such "skinned" fibers, kinetic (permeability) evaluation of static structure such as mean pore size is not realistic and is further generalized to the term "equivalent pore size."

INTRODUCTION

We have recently reported on the spinning and properties of porous polysulfone hollow fibers (PSHF).[1-3] The fibers were spun to withstand external hydraulic pressures of more than 1000 psi and to provide hydraulic permeabilities of more than 10^{-4} cm/sec atm. The porous hollow fiber can be used in a variety of ultrafiltration applications and as support for ultrathin semipermeable membranes. The functional utility of the fibers is dependent upon their porosity and pore dimensions. However, some ambiguities are generally involved in pore size definitions. Cast membrane or spun fibers display a wide range of pore size distributions when compared to the fine cylindrical capillaries that extend from wall to wall in Nucleopore membranes. Such membranes are prepared by chemically etching the tracks of charged particles that are passed through polycarbonate fiber.[4] The morphology of the spun polysulfone hollow fiber walls comes closer to that of a consolidated material.[3,5] As such, clear-cut definition of the "pore" geometry is not available. There are several factors that determine the functionality and the efficiency of porous materials. Among these are the mean pore size, pore size distribution, tortuosity, and effective porosity. Effective porosity is defined as the density, or distribution per space unit, of open

pores which extend from wall to wall of a fiber.   This definition specifically excludes consideration of closed cell pores.   Porosity is a parameter of major importance.   Its evaluation becomes very complicated when the spinning (or casting) formulation produces a nonisotropic fiber, e.g., a fiber with dense skin on the interface of the porous wall structure.   For such cases, the mean pore size determined by dynamic measurements[5] may lose its true geometric meaning. For this reason, "equivalent pore size" is the preferred term for any kinetic measurement of porosity.

The present manuscript reports the porosity of the polysulfone hollow fiber as measured by kinetic methods (gas permeation) and electron microscopy.   The fibers reported here were spun from a ternary component mixture:[2]   polysulfone (PS)–poly(vinylpyrrolidone) (PVP)–dimethylacetamide (DMA).   The nascent fiber was quenched by water, which causes coagulation.   The quenched polymers then phase separate, and the PVP is dissolved into the precipitant water.   We have shown previously[3] that the introduction of PVP to the spinning dope helps to eliminate the formation of dense skin on the fiber surface and contributes to the wall porosity.

Surface pore characteristics are another specific issue of importance.   The surface pore size is a determining factor if the fiber is to be used to support an ultrathin membrane.   The surface pores can be altered toward a desired size by posttreatment of the fiber, as discussed below.

EXPERIMENTAL

Polysulfone Hollow Fiber (PSHF)

The spinning procedure of the polysulfone hollow fiber was described and discussed thoroughly in previous publications.[2,3]   Briefly, the fibers were spun from a solution of polysulfone (PS) and poly(vinylpyrrolidone) (PVP) in dimethylacetamide (DMA).   The fibers were produced by a tube-in-jet spinning technique, using the dry-wet (sometimes called dry jet-wet)[3] process.   In this procedure, the fibers were spun into a gas phase and subsequently were quenched in a water bath.

Preparation of Polysulfone Hollow Fibers for Scanning Electron Microscope (SEM)

Polysulfone hollow fibers were attached to aluminum disks with a double-surface Scotch tape.   Cross sections of polysulfone hollow fibers were prepared for the SEM by breaking the fibers at the temperature of liquid nitrogen.   Quick freezing of the fiber to such a temperature does not damage the fiber and leaves an undeformed surface.   The mounted specimen was then shadowed (coated) with gold.

Gas Permeability and Evaluation of the Equivalent Pore Size Radius (m)

The principles of gas permeability measurements have been described precisely by Yasuda and Tsai.[6]   This method was modified for hollow fibers in the present
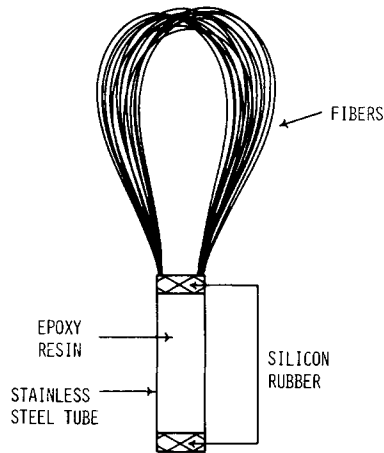
Fig. 1. Hollow fiber bundle.

study, so that there was no need to consider the permeability through the membrane support, as in Yasuda's studies.

The arrangement of fiber bundles for gas permeation measurement is shown in Figure 1. The experimental setup for hollow fiber gas permeation is shown in Figure 2. The method is based upon gas pressure decay in a reservoir. The operation takes the following steps: Gas from the supply cylinder is allowed to flow through the system, i.e., permeate through the fiber's wall until steady-state flow is detected by the flow meter (item 7, Fig. 2) and pressure of 120 psi is maintained in the system. Valve 2 is then closed quickly before pressure falls to 100 psi. (The preceding step is required to avoid the initial transient stage of pressure decay.) The pressure decay curve is recorded, its slope is measured, and the slope at various pressures is calculated.

The data required for the permeability calculations include: V_0, the volume of the entire system (from valve 2 to the fibers, Fig. 2); the tested fiber area; and
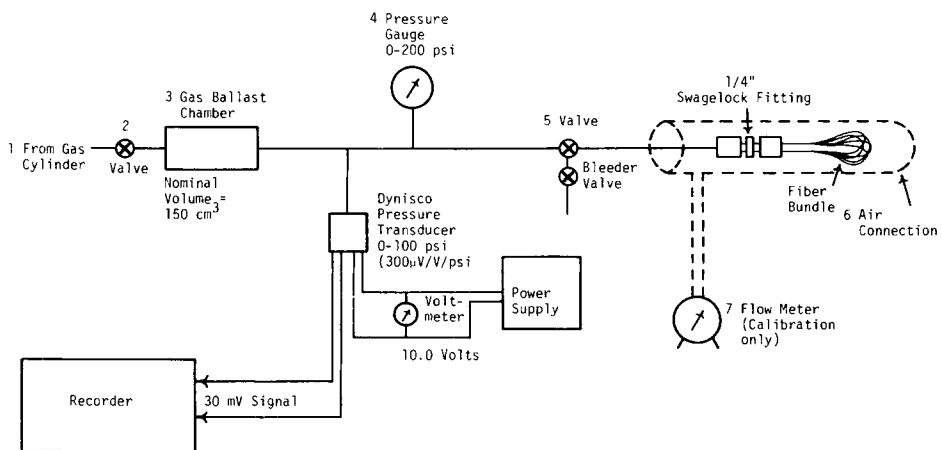

Fig. 2. Experimental setup for hollow fiber gas permeation.

the pressure in the reservoir as a function time.   The fixed volume V_0 can be identified as the constant of proportionality in the expression

$$Qp' = V_0(dp/dt) \qquad (1)$$

where dp/dt is the pressure drop, p' is outlet pressure, and Q is volume flow rate at pressure p', measured in our apparatus with a flow meter.

Bundles containing fibers 70 in. long were used in these measurements.   Five permeability runs were performed on each bundle.   At least three replicate bundles of each fiber type were prepared and measured.

The following theoretical considerations apply to the calculation of the mean pore ratio of polysulfone hollow fibers: The gas flux J through the fibers can be expressed by the flux equation

$$J = K \frac{\Delta p}{l} \qquad (2)$$

where K is the permeability coefficient (cm^2/sec), Δp is the pressure difference across the wall, and l is the wall thickness.   The experimental setup shown in Figure 2 allows determination of K from the equation

$$K = \frac{l}{A} \frac{p'}{\Delta p} Q \qquad (3)$$

The denominator A is the area of the fibers (which is calculated from $A = n\pi \bar{D}L$), where n is the number of fibers and L is their length; $\bar{D}$ is the average diameter of the fiber, i.e., $\bar{D}$ is the inside diameter D + thickness l; and p' is the discharge pressure (atmospheric pressure in our experiment).   The expression Qp'/A is
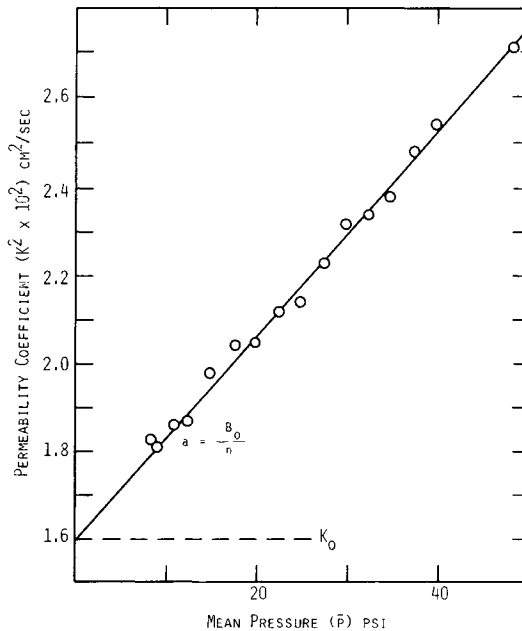

Fig. 3. Permeability coefficient (of N_2) vs. mean pressure in polysulfone hollow fibers: $K_0 = 1.6 \times 10^{-3} cm^2/sec$; $a = 2.3 \times 10^{-5}$ $cm^2/sec\text{-}psi$.

equivalent to J and is expressed in units of volume flow, dyn/cm sec. The designations J and Q indicate whether the volume flux rate[5] determined from the pressure decay in the gas ballast chamber (item 3, Fig. 2), as by Yasuda and Tsai,[6] or from the volume flow rate (Q) measured by flow meter (item 7, Fig. 2). In order for J to equal Qp'/A, these values must be determined at the same pressure or must be corrected to the same pressure.

The permeability coefficient K of a porous medium can be expressed by

$$K = K_0 + \frac{B_0}{\eta}\bar{p} \tag{4}$$

where K_0 (cm^2/sec) is the Knudsen permeability coefficient, η is the viscosity of the gas (sec/cm^2), and $\bar{p}$ the mean pressure on both sides of the membrane, $(p_1 + p_2)/2$. The term B_0 (cm^2) is the geometric factor of the medium. Values of K_0 and B_0 can be calculated from a plot of K versus $\bar{p}$ as shown in Figure 3.

It has been shown[6] that the porosity ϵ and the tortuosity factor q can be related to K_0 and B_0 by the equations

$$K_0 = \frac{4}{3}\left(\frac{\delta}{k_1}\right)\left(\frac{\bar{v}}{q^2}\right)\epsilon m \tag{5}$$

$$B_0 = \left(\frac{m^2}{k}\right)\left(\frac{\epsilon}{q^2}\right) \tag{6}$$

Carman[5] postulates that δ/k_1 and k are constant (0.8 and 2.5, respectively) for all porous membranes. The average molecular velocity ($\bar{v}$) of gas of molecular weight M is given by

$$\bar{v} = \left(\frac{8RT}{\pi M}\right)^{1/2} \tag{7}$$

The equivalent pore radius m can be calculated by combining eqs. (5), (6), and (7):

$$m = \frac{16}{3}\left(\frac{B_0}{K_0}\right)\left(\frac{2RT}{\pi M}\right)^{1/2} \tag{8}$$

This equation was used by Yasuda and Tsai to calculate the pore size of flat polysulfone porous membrane. In the measurement of flat sheet membranes, those authors found it necessary to support the membranes by rigid, porous media. Such measurements require the derivation of expressions which distinguish between the resistance of the membrane under evaluation and the resistance of the support. Thus the analysis must, in effect, deal with a composite membrane. The problem of measurements with hollow fibers is simpler because the fiber wall is self-supporting. The ability to operate without a composite structure is an advantage unique to the hollow fiber membranes.

In practice, when nitrogen is used as the gas in the measurements, eq. (4) is rederived (for use at 298°K) to yield

$$B_0 = (2.58 \times 10^{-9}\text{ psi-sec}) \cdot a \tag{9}$$

where $a = B_0/\eta$ and is determined as shown in Figure 3.

Thus, for measurement with nitrogen,

$$m = (1.266 \times 10^5\text{ cm/sec})\, B_0/K_0 \tag{10}$$

and

$$\frac{\epsilon}{q^2} = \frac{2.5B_0}{m^2} \qquad (11)$$

(Any unit of pressure can be used in the calculation as long as the appropriate conversion factor is included. The viscosities of gases are often given in units of dyne sec/cm^2 = poise; the conversion factor to psi units is dyne/cm^2 = 1.45 × 10^{-5} psi.)

Maximum Pore Size Determination

Maximum pore size (m_x), as distinguished from equivalent pore size, can be determined by "bubble breakthrough measurements." The pressure p required to remove a fluid from a pore, when the walls of the pore are wetted by the fluid, is given by the expression[7]

$$p = \frac{2\gamma}{m_x} \qquad (12)$$

where γ is the surface tension of the liquid that occupied the pore.

The fiber bundle was impregnated with a relatively low surface tension liquid, such as isopropanol, by immersion until the walls of the fibers' pores were wetted. A stream of nitrogen was pressurized in the core of the immersed fibers. The recorded pressure at which gas bubbles first appeared through the fiber wall is used in eq. (12) for the determination of m_x.

Water Flux Measurements

Ultrafiltration rates were determined by steady-state measurement of the quantity of water permeating a fiber bundle at 0.4 atm. The fiber bundles were prepared as for the pore size determinations. Approximately 100 fibers were potted into either a ½-in.-diameter polypropylene tubing or a ⅜-in. steel tubing. Swagelock fittings were used to connect the experimental bundle to the pressurized water supply. A 10-ml buret between the N$_2$ bottle and the fiber bundle was used for measuring the water flux.

The hydraulic permeability L_p of the polysulfone hollow fiber is calculated from the flux equation

$$J = L_p \, \Delta p \, A \qquad (13)$$

where J is flow rate (cm^3/sec), A is area (cm^2) of the measured polysulfone hollow fiber, and Δp is differential pressure applied (atm). The units of L_p are cm^3/cm^2 sec atm.

Void Volume Determination

The void volume measurements are based on the gravimetric analysis of water entrapped in the voids of the fiber walls. To calculate the void volume, the weight of water and the weight of dry fiber are determined after a water-equilibrated fiber sample is centrifuged to remove surface water and internal bore-occluded water. The centrifugation is done with the fibers supported, on end,

on a wire mesh support in the centrifuge tube. After centrifugation, the wet fiber is weighed; the sample is then dried at 105°C and reweighed. The void volume is calculated from

$$\text{void volume} = \frac{\left(\dfrac{\text{wt}}{\rho}\right)_{\text{H}_2\text{O}}}{\left(\dfrac{\text{wt}}{\rho}\right)_{\text{H}_2\text{O}} + \left(\dfrac{\text{wt}}{\rho}\right)_{\text{polymer}}} \times 100 \tag{14}$$

where wt and ρ represent mass and density, respectively, and the subscripts indicate the phase.

RESULTS AND DISCUSSIONS

Pore Size and Microstructure of Polysulfone Hollow Fibers

The equivalent pore sizes of a fiber can be related to the polymer content in the spinning solution and to the spinning conditions.[2,3] Many of the parameters which determine the fiber's macrostructure are also variables in the microstructure formation.[3] Scanning electron micrographs of some characteristic structures are shown in Figures 4–7. Subtle changes of the wall microstructure (Fig. 4), and in surfaces-forming very thin, porous or nonporous skins (Fig. 7), are observable only by use of the scanning electron microscope. The fibers of Figures 4–6 were spun from a solution of 250,000 cP (50°C) with a PS/PVP ratio of 3/2 (w/w). The fiber shown in Figure 7 came from a solution of only 11,000
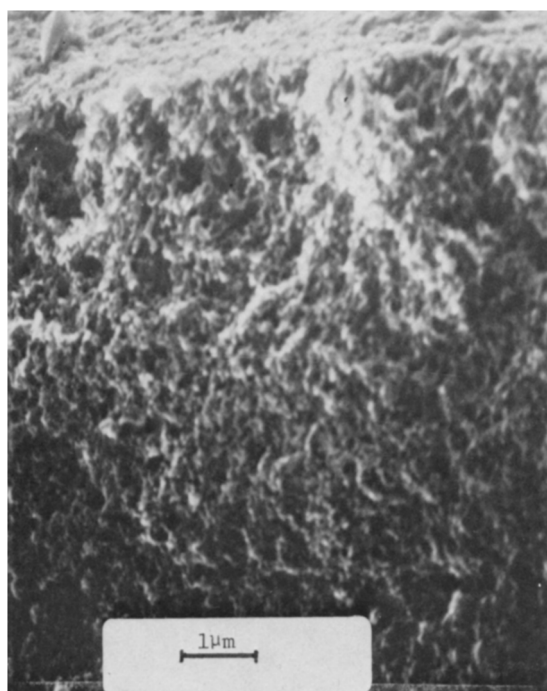

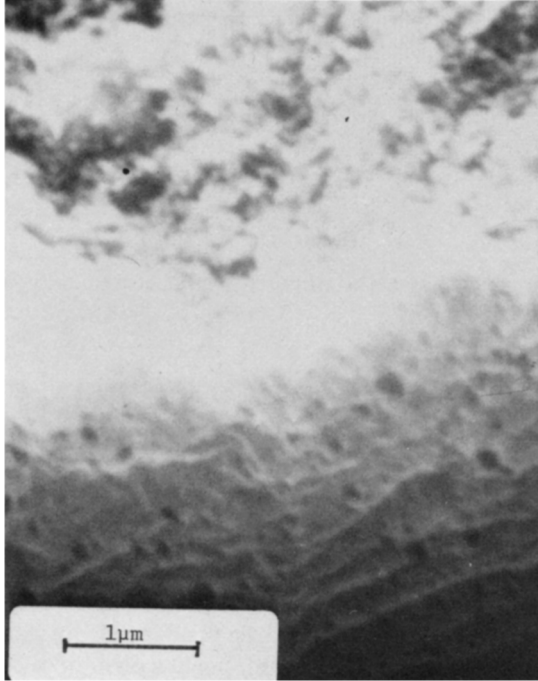Fig. 4. Wall morphology of polysulfone hollow fiber (oven dried 110°C, 10 min).

Fig. 5. Bore wall surface structure of the fiber shown in Fig. 4.
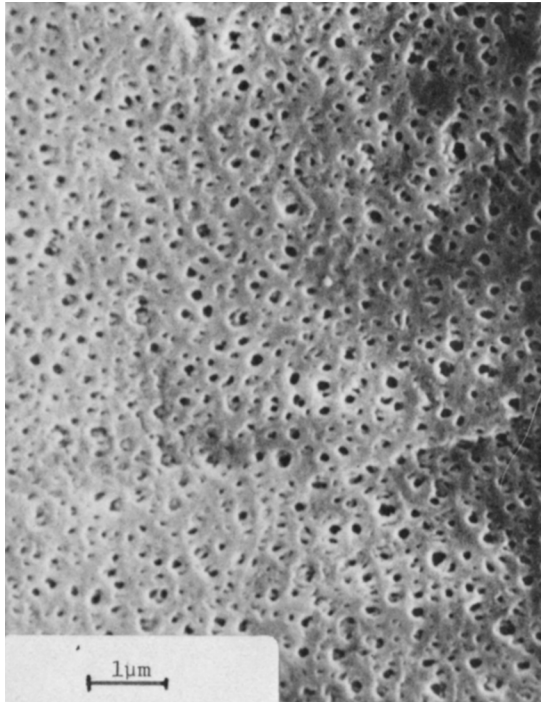

Fig. 6. External surface of hollow fiber that was spun from polysulfone/PVP (3:2) solution in DMA.
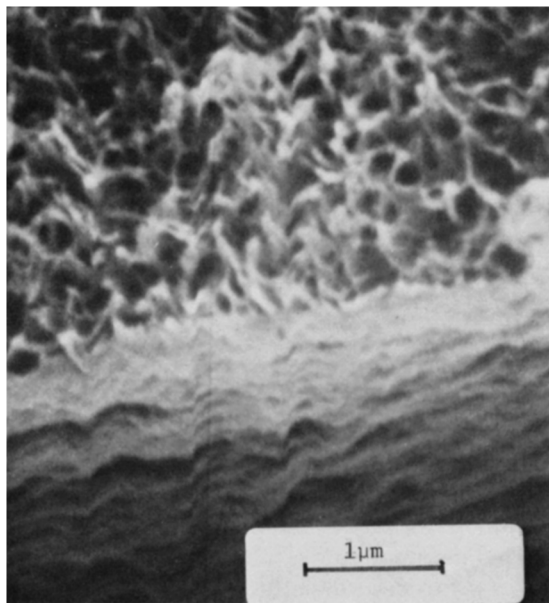
Fig. 7. Dense external "skin" (less than 250 Å thick) on a spongy wall structure of polysulfone hollow fiber.

cP (50°C) and was spun with no PVP. The spinning solutions of both types of fiber contained the same quantity of polysulfone. Although the fiber in Figure 7 displays a much more open microstructure within its wall, its hydraulic permeability is only 5% of that of the fibers shown in Figures 4–6. This comparison illustrates the interaction of the fiber microstructure on the coagulation/extrusion conditions. The lower hydraulic permeability of the fiber shown in Figure 7 can be attributed to the density of its surface "skin."

The porosity of a membrane is often identified with its inherent ability to permit permeation of solutes under suitable driving forces. From gas permeation and/or liquid permeation rates, one can make deductions about the porosity and equivalent pore size of the membrane. The use of the gas permeation techniques described above allow estimation of the contiguous pore volume and provide an estimate of average physical pore size. The use of imbibed water allows an estimate of the total void volume, including the volume of closed, or dead-end, voids.

It must be recognized that permeability coefficients are phenomenological parameters and that they can be interpreted into physical dimensions only with reservation. The equivalent pore size m is a defined quantity which may not be observable by microscopy; the terms porosity ϵ, tortuosity q, and pore radius m are kinetic parameters. The description of nonuniform structural components, i.e., skin depth (Figs. 5 and 7), dead-end pores, pore density gradients, etc., by such parameters is not realistic, since there may be no consistent relationship between the physical interpretation and the observed phenomenological constants.

The kinetically derived parameters can, however, be viewed as the operationally significant values, since the morphology which leads to these values also

TABLE I
Fiber Pore Size and Effective Porosity of Polysulfone Hollow Fiber

Fiber designation	Wall thickness, μm	Calculated equivalent pore size, m, μm	Maximum pore size, μm	Effective porosity, $(\epsilon/q^2) \times 10^2$	Hydraulic permeability $L_p \times 10^5$, cm/sec-atm
13-1	101	0.025	0.11	0.26	70
14-1	143	0.038	0.09	4.6	150
19-1	116	0.040	0.11	1.5	32
19-2	100	0.040	0.08	1.1	36
1-1	90	0.040	0.11	2.8	48
1-2	125	0.030	0.10	1.2	52
4-1	100	0.030	0.08	1.1	58
8-3	82	0.053	0.09	2.8	93
11-1	71	0.053	0.09	0.9	61

determines the functional utility of the fibers. In that context, ϵ, q, and m describe the operational permeability.

The term ϵ/q^2 is used to describe effective porosity. Equations (5) and (6) do not provide means to calculate ϵ and q independently; thus, the ratio ϵ/q^2 is used to provide comparisons. Practically, as the value of ϵ/q^2 increases, the effective porosity increases. However, such an increase does not require a corresponding increase in permeability, since the permeability coefficient is also a function of m, as shown by combining eqs. (4) and (6) to yield

$$K = K_0 + \frac{\bar{p}m^2}{2.5}\,(\epsilon/q^2) \tag{15}$$

To summarize the relationship between static and kinetic descriptions of porosity, it can be stated that only contiguous pores register in kinetic measurements. The smaller the tortuosity, the more efficient will be the transport through the pores. The average dimension m measured by gas permeation has no geometric meaning, especially for anisotropic membranes, or for nonuniform membranes such as seen in Figure 7.

In Table I are shown mean and maximum pore sizes of some polysulfone hollow fibers. It should be noted that the bubble method that was utilized to measure the maximum pore size has a more pronounced geometric value than m, since it is a measure of the largest capillary radius; this is true for nonisotropic membranes also.

The L_p values given in Table I reflect the water permeability of the fiber walls. In this table, the highest value of ϵ/q^2 (sample 14-1) provides also the highest value of L_p. In view of the fact that this sample also had the thickest wall, the intrinsic permeability is even higher than the comparisons imply, since the values are not corrected for wall thickness.

However, as shown above, the ratio of ϵ/q^2 is not the only determinant of water flux. Comparison of samples #8-3 and #1-1, both of which have similar values of ϵ/q^2, shows that the larger mean pore size sample is also the fiber with the highest L_p. Thus, both pore size and effective porosity contribute to water permeability.

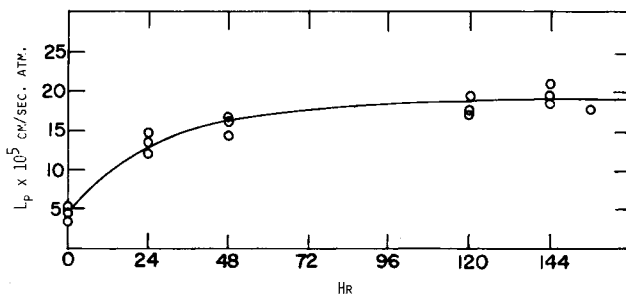Other factors also are involved in comparisons of gas and liquid permeabilities.

Fig. 8. Rate of hydraulic permeability regain of previously air dried (21°C) polysulfone hollow fiber equilibrated in water.

The wetting properties of the polymer determine the largest pores which will be filled with liquid at a given pressure, but gas measurements are not influenced by the size of such pores. The equilibrium water content of the dense polymer may have a swelling effect on very small pores during the liquid permeation measurements. Residual additives such as PVP, solvent, etc., may influence the interfacial tension between the polymer and the liquid and thus bias the results. Thus, one cannot rely on only the pore size and porosity for complete prediction of the variables which determine L_p. Apropos of the above discussion, it was found that the hydraulic permeability of a fiber which has been dried carefully is substantially less than that of a fiber which is kept wet after spinning. As shown in Figure 8, it requires more than 48 hr for dry fiber that is immersed in water to regain a constant L_p value.

We have found linear correlation between $\log L_p$ and $\log e/q^2$, as seen in Figure 9. This correlation may result from the fact that the samples represent mor-
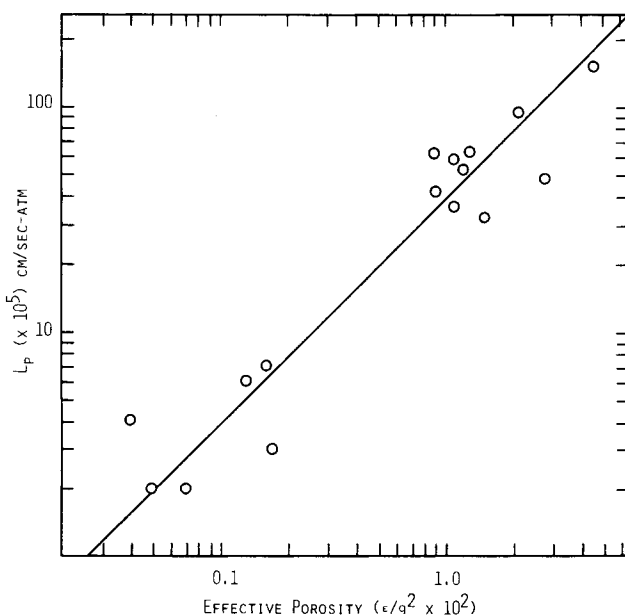

Fig. 9. Hydraulic permeability vs. effective porosity of wet polysulfone hollow fibers.

CABASSO ET AL.

<div align="center">TABLE II</div>
<div align="center">Relation of Fiber Porosities and Hydraulic Permeabilities</div>

Effective porosity, $(\epsilon/q^2) \times 10^2$	Calculated Equivalent Pore Size m, μm	Void volume, %	Hydraulic Permeability $L_p \times 10^5$, cm/sec-atm
4.6	0.038	75.6	150
2.8	0.040	73.2	48
2.1	0.053	75.9	93
1.5	0.040	74.2	32
1.1	0.040	70.6	36
0.9	0.075	73.4	42
0.17	0.030	69.1	3
0.03	0.087	65.1	6
0.07	0.033	58.4	2

phologies which have equivalent pore sizes of the same order of magnitude; i.e., the differences in m may not be significant enough to cause large deviations.

Void Volume and Porosity

The void volume of a porous membrane is defined as the fraction of the membrane volume which is not occupied by the polymer. Thus, if all the pores are interconnected (no dead ends), the entire void volume participates in transport. The data in Table II indicate that large changes in the void volume
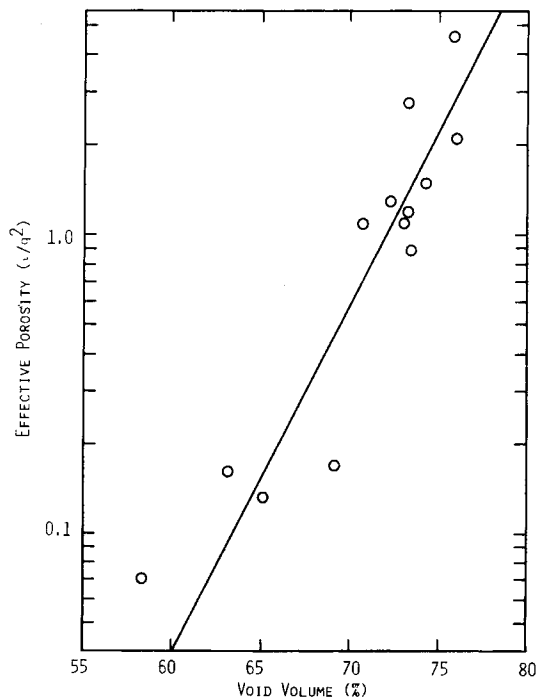

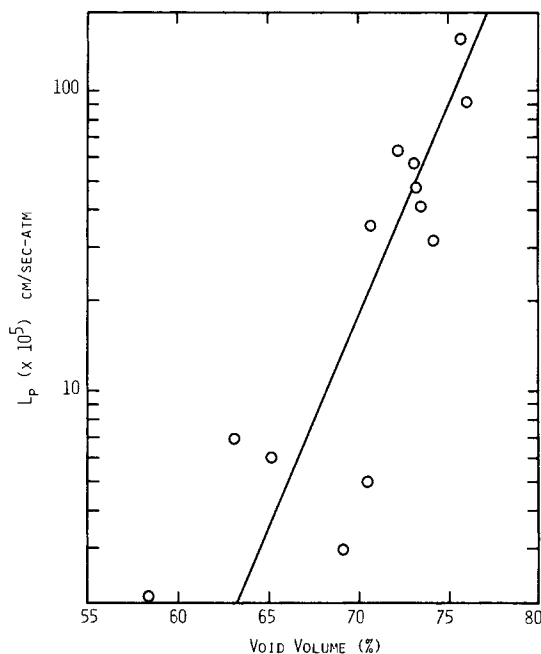Fig. 10. Effective porosity vs. void volume in polysulfone hollow fibers.

Fig. 11. Hydraulic permeability vs. void volume in polysulfone hollow fibers.

do not systematically affect the equivalent pore size; however, there is a correlation between ϵ/q^2 and the void volume as shown in Figure 10.

The low value of ϵ/q^2 compared to those of the void volume indicate either a very high tortuosity factor, or a large number of dead-end pores. In the first sample shown in Table II, the ratio between the void volume and the effective porosity ϵ/q^2 is equal to 16.4. If no dead-end pores existed in this fiber, the tortuosity factor q^2 would have been 16.4, an extremely high value considering that the tortuosity factor of a consolidated spherical material is assumed to be ≤ 2 from statistical considerations.[5] If, however, we assign to q^2 a value of 2, it implies that 66.4% of the void volume is not active in any transport through the fiber walls. This is a typical situation for an anisotropic membrane which has dense domains, or skin structures as illustrated in Figure 7. It should be noted that the linear relations in Figures 9 and 10 must lead to a linear relation between $\log L_p$ and the void volume (Fig. 11). This empirical relationship has practical meaning since small changes in the void volume of the polysulfone hollow fiber lead to large increases in hydraulic permeability while the mechanical properties of the fiber are not drastically altered. The ratio of effective to total void volume corresponds in its magnitude to reduction in apparent diffusion coefficients of small solutes through water-filled pores in membranes.[8]

Comparison with Flat Sheet Membranes

Flat porous polysulfone membranes are cast and quenched[6,9] under different conditions from those employed in fabricating the polysulfone hollow fibers. In flat sheet casting, a relatively low concentration (15 ± 2 wt %) of polysulfone is used; in some cases, this is only half of the concentration used for the fiber
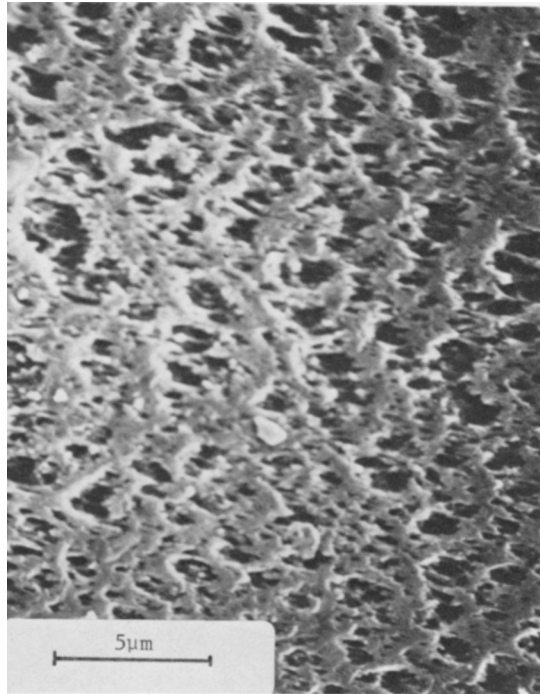
Fig. 12. Surface pore structure of an ambient dried (21°C) polysulfone hollow fiber.
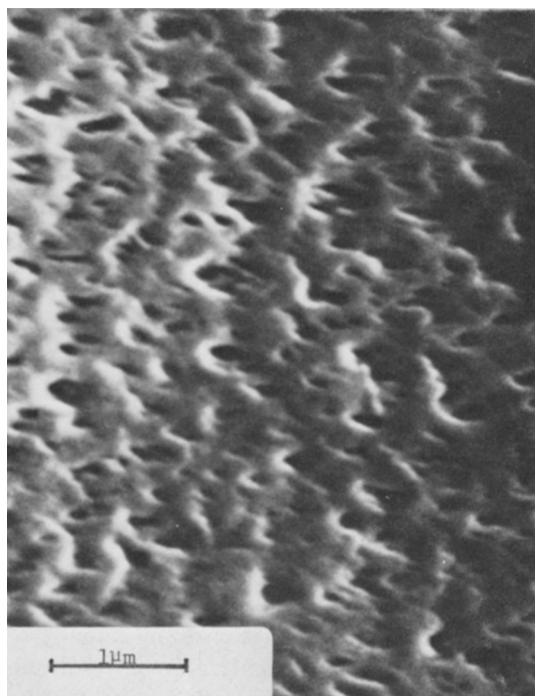

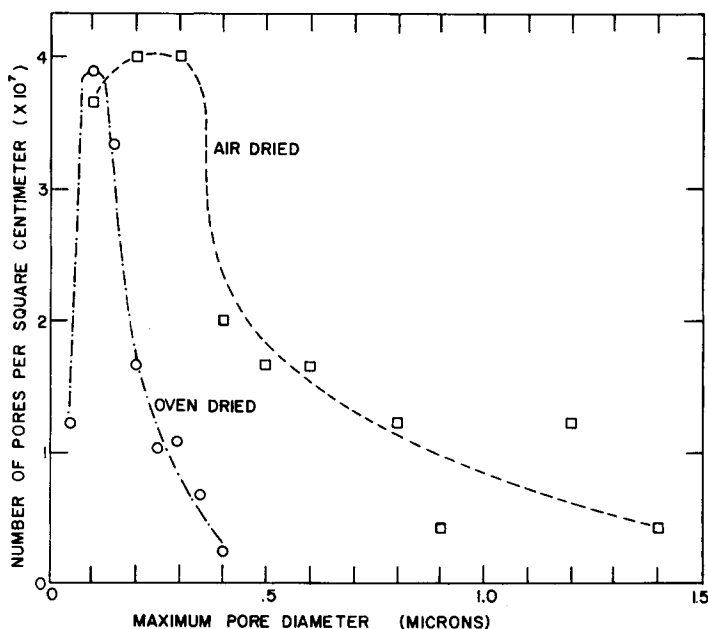Fig. 13. The same fiber shown in Fig. 12 oven dried 110°C for 10 min.

Fig. 14. Pore density vs. pore diameter of heat-dried (110°C, 10 min) and ambient-dried (21°C) polysulfone hollow fiber.

spinning solution. The most pronounced morphologic difference between the flat sheet and hollow fiber is shown in the values of the effective porosity ϵ/q^2. Effective porosities range between $\epsilon/q^2 \times 10^2 \simeq 10$–40 for the flat membranes.[6] These values are almost one order of magnitude higher than those shown in Table II and Figure 10 for polysulfone hollow fibers. However, the average pore dimensions of fiber, as measured by the gas permeability method, are of the same order of magnitude for both the fibers and for the flat membranes.

Structure of Surface Pores

Typical external surface structures of polysulfone hollow fibers are shown in Figure 6. Internal surfaces are shown in Figure 5. The surface structure (internal or external) can be modified according to the spinning solution composition and the spinning conditions, as shown in previous publications.[1-3] The importance of the surface morphology is to be emphasized in cases in which the polysulfone hollow fiber has to support an ultrathin membrane under high pressure, e.g., for reverse osmosis,[1] or for ultrafiltration applications. In such a case the membrane to be deposited has to be fabricated so that its thickness is compatible with the pore dimensions of the supporting surface pore dimensions of the supporting surface and the maximum dydraulic pressure to be experienced. The porous skinned fiber that is shown in Figures 5, 6, 12, and 13 displays SEM-observable pore diameters of 0.1–1.5 μm.

Typical distribution curves of the pore diameter are shown in Figures 14 and 15. Pores with diameters less than 0.01 μm are not detectable by the SEM method used by the present study. (The use of methyl cellulosolve in the spinning composition instead of PVP, or a change of the spinning conditions,
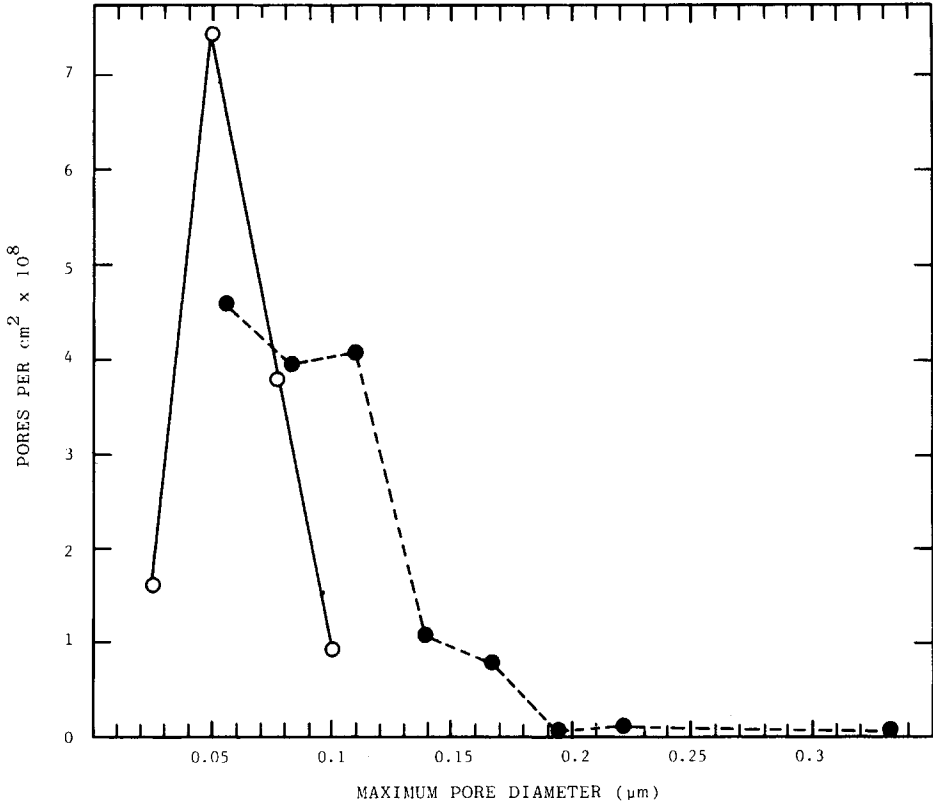
Fig. 15. Pore density vs. pore diameter of heat-dried (110°C, 10 min) and ambient air-dried (21°C) polysulfone hollow fiber: (O) head heated; (●) unheated.

may produce surfaces with pore dimensions that display a maximum diameter of less than 0.01 μm.)

In order to study the effect of drying and heat-cycling on the surface porosity of the fibers, they were exposed to drying and heat treatment.   It was found that
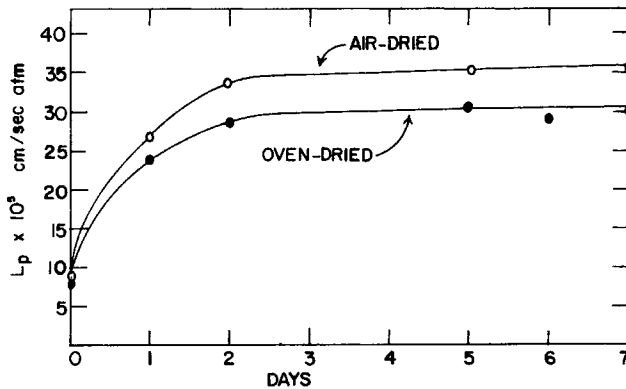

Fig. 16. Rate of hydraulic permeability regain of previously oven-dried (110°C, 10 min) and air-dried (21°C) polysulfone hollow fibers in water.

such treatments decreased the hydraulic permeabilities. In the spinning procedure, the nascent fiber is quenched by water and is stored wet. When the fiber is dried at ambient temperature, it takes at least 48 hr for the rewetted fiber to regain a constant hydraulic permeability, as shown in Figure 8. Heat treating the fiber (by drying it at 110°C in an air-circulating oven) narrows the range of the pore size distribution of the fiber (Figs. 12–15). The reduction in surface pore size that occurs as a result of such treatment cannot be explained by the fiber shrinkage. The overall fiber dimensions (length and diameter) are reduced by only 1% by heat treatment at 110°C. However, the pore diameters, as shown in Figures 12–15, are reduced by almost one order of magnitude.

The hydraulic permeability of a heat-treated fiber, as compared to that of an untreated fiber, exhibits similar trends, as shown in Figure 16. The decrease in the ultimate L_P for heat-treated fiber is only ~14%. The small changes of the fiber dimensions and hydraulic permeabilities compared to the large changes in the surface pore dimensions can be explained if "polymer flow" occurs at the surface. This point has not been resolved. However, several other observations do support this possibility. The most important of these observations is that the surface layer is very thin, as shown in Figures 5–7, and displays, for many of the spun fibers, a smaller pore density than the interior.

Surface structure and surface treatment, especially as related to problems of coating ultrathin membranes, will be discussed in subsequent works.[10]

CONCLUSIONS

It has been demonstrated that spun hollow polysulfone fibers have complex structures. The morphologies must be understood in terms of discrete structures at the surface, as opposed to the interior of the fiber wall. It has also been shown previously[2,3] that these morphologies are systematically related to the conditions under which the fibers are spun. Some characteristics of the structure can be significantly altered by handling of the fibers after spinning (such as heating and drying). These changes may be of either a transient or permanent nature. Regardless of whether these changes affect the functional utility of the fibers, they must be taken into account in measurements of the fiber properties.

The equivalent pores size parameter is readily measurable by the method described herein. When the results of SEM analysis of the surface structures are combined with equivalent pore size measurements, a meaningful determination of fiber "porosity" can be achieved.

References

1. I. Cabasso, E. Klein, and J. K. Smith, *Org. Coat. Plast. Chem. Prepr.,* **35,** 492 (1975).
2. I. Cabasso, E. Klein, and J. K. Smith, *J. Appl. Polym. Sci,* **20,** 2377 (1976).
3. I. Cabasso, E. Klein, and J. K. Smith, *J. Appl. Polym. Sci.,* **21,** 165 (1977).
4. R. Fleischer, P. Price, and R. Walker, *Ann. Rev. Nucl. Sci.,* **15,** 1 (1965).
5. P. G. Carmen, *Flow of Gas through Porous Media,* Butterworth, London, 1956.
6. H. Yasuda and J. T. Tsai, *J. Appl. Polym. Sci.,* **18,** 805 (1974).
7. R. E. Kesting, *Synthetic Polymer Membranes,* McGraw-Hill, New York, 1971, p. 29.

8. E. Klein, J. K. Smith and F. F. Holland, in *Permeability of Plastic Film and Coatings,* H. B. Hopfenberg, Ed. Plenum Press, 1975, p. 423

9. J. E. Cadotte and L. T. Rozelle, Progress Report on In Situ-Fomed Condensation Polymers for Reverse Osmosis Membrane to the Office of Saline Water (U.S. Dept. of Inter.) Contract No. 14-30-2883, 1972.

10. I. Cabasso, J. K. Smith, and E. Klein, in preparation.